

Original citation:

Latko-Durałek, Paulina, Macutkevic, Jan, Kay, Christopher James, Boczkowska, Anna and McNally, Tony. (2017) Hot-melt adhesives based on co-polyamide and multiwalled carbon nanotubes. *Journal of Applied Polymer Science*. p. 45999

Permanent WRAP URL:

<http://wrap.warwick.ac.uk/95179>

Copyright and reuse:

The Warwick Research Archive Portal (WRAP) makes this work by researchers of the University of Warwick available open access under the following conditions. Copyright © and all moral rights to the version of the paper presented here belong to the individual author(s) and/or other copyright owners. To the extent reasonable and practicable the material made available in WRAP has been checked for eligibility before being made available.

Copies of full items can be used for personal research or study, educational, or not-for profit purposes without prior permission or charge. Provided that the authors, title and full bibliographic details are credited, a hyperlink and/or URL is given for the original metadata page and the content is not changed in any way.

Publisher's statement:

"This is the peer reviewed version of the following Latko-Durałek, Paulina, Macutkevic, Jan, Kay, Christopher James, Boczkowska, Anna and McNally, Tony. (2017) Hot-melt adhesives based on co-polyamide and multiwalled carbon nanotubes. *Journal of Applied Polymer Science*. p. 45999 which has been published in final form at <http://dx.doi.org/10.1002/app.45999> . This article may be used for non-commercial purposes in accordance with [Wiley Terms and Conditions for Self-Archiving](#)."

A note on versions:

The version presented here may differ from the published version or, version of record, if you wish to cite this item you are advised to consult the publisher's version. Please see the 'permanent WRAP URL' above for details on accessing the published version and note that access may require a subscription.

For more information, please contact the WRAP Team at: wrap@warwick.ac.uk

Hot-Melt Adhesives based on Co-polyamide and Multi-Walled Carbon Nanotubes

Paulina Latko-Duralek^[1,2], Jan Macutkevic^[3], Christopher Kay^[4], Anna Boczkowska^[1,2]

Tony McNally^[5]

^[1] Faculty of Materials Science and Engineering, Warsaw University of Technology -Woloska 141,
02-507 Warsaw, Poland

^[2] Technology Partners Foundation- Pawinskiego 5A, 02-106 Warsaw, Poland

^[3] Vilnius University, Sauletekio al. 9, Vilnius 10222, Lithuania

^[4] Department of Chemistry, University of Warwick, CV4 7AL, UK

^[5] International Institute for Nanocomposites Manufacturing (IINM), WMG, University of Warwick, CV4
7AL, UK.

Corresponding author: paulina.latko@inmat.pw.edu.pl

Faculty of Materials Science and Engineering, Warsaw University of Technology -Woloska 141,
02-507 Warsaw, Poland

Abstract:

Composites of two hot melt adhesives based on co-polyamides, one high viscosity (coPA_A) the other low viscosity (coPA_B) and, multi-walled carbon nanotubes (MWCNTs) were prepared using twin-screw extrusion via dilution of masterbatches. Examination of these composites across the length scales confirmed the MWCNTs were uniformly dispersed and distributed in the polymer matrices, although some micron size agglomerations were also observed. A rheological percolation was determined from oscillatory rheology measurements at a mass fraction of MWCNTs below 0.01 for coPA_B and, between 0.01 and 0.02 for coPA_A. Significant increases in complex viscosity and storage modulus confirmed the 'pseudo-solid' like behaviour of the composite materials. Electrical percolation, determined from dielectric spectroscopy was, found to be at 0.03 and 0.01 MWCNT mass fraction for coPA_A and coPA_B based composites, respectively. Addition of MWCNTs resulted in heterogeneous nucleation

and altered the crystallization kinetics of both copolymers. Indirect evidence from contact angle measurements and surface energy calculations confirmed that MWCNT addition enhanced the adhesive properties of coPA_B to a level similar to coPA_A.

1. Introduction

There continues to be intense research interest in the preparation and properties of composites of polymers and multi-walled carbon nanotubes (MWCNTs) in the anticipation that the addition of MWCNTs to polymer matrices will result in the development of functional composite materials with new industrial applications. MWCNTs mainly due to their excellent mechanical properties, electrical and thermal conductivity combined with relatively low density offer great potential for the exploitation of MWCNT filled polymers in electronic, automotive, aerospace and bioengineering applications ¹. Many thermoplastic polymers have been filled with MWCNTs using various preparation techniques including, *in-situ* polymerization ², calendaring ³, solution mixing methods ⁴, spinning ⁵ and melt mixing ⁶⁻¹⁷, the latter because this process has widespread use in industry.

Within melt mixing methods, two routes are possible. The first is direct mixing of powder MWCNTs with the polymer, second by dilution from a highly concentrated masterbatch by the neat polymer to the desired MWCNT loading. These methods differ in the ultimate level of MWCNT dispersion and distribution achievable. In the first route, primary MWCNT agglomerates are introduced to the polymer first via wetting, then infiltration (by the polymer macromolecules), rupture and/ or erosion due to the destruction of MWCNT agglomerates by breaking into smaller sizes and possibly to

sections of single nanotubes ⁶. The masterbatch route includes the dilution of a masterbatch with a high concentration of MWCNTs by the same polymer as used in the masterbatch to produce composites with lower MWCNT concentrations. In general, better dispersion is achieved for high concentration filled (nano)composites (masterbatch) due to the favourable shear forces employed during melt-mixing,⁷ although this has been poorly studied for most polymer nanocomposites. After dilution the MWCNT dispersion is improved but still some MWCNTs agglomerates remain in the composite material ⁸. From a technical and practical point of view, the masterbatch route is safer because it excludes the use of powder MWCNTs and eliminates potential environmental and health and safety hazards ⁹. Many processing parameters associated with the melt-mixing process have an effect on the different states of MWCNTs dispersion and distribution in polymer matrices, all governing the final properties of the (nano)composite material. These include: i) polymer structure (melt viscosity, molecular weight, ratio of amorphous to crystalline content) ¹⁰ ii) processing conditions (temperature profile, screw velocity and configuration, mixing time, feeding conditions ¹¹⁻¹³ and iii) CNT type (geometry, functionality, purity) ¹³. All these factors influence the value for rheological and electrical percolation threshold which are related to the restriction of polymer chain mobility by MWCNTs and the formation of an interconnected CNT-CNT conductive network ¹⁴. For most thermoplastic based (nano)composites, fabricated by melt-mixing, the electrical percolation threshold is attained typically between 1 wt% and 5 wt% MWCNTs ¹⁵, although values as low as 0.07 vol% have been reported for melt mixed systems ¹⁶.

In contrast, low molecular weight hot melt adhesives (HMAs) filled with MWCNTs have received much less attention. From the reviews ²⁰⁻²¹, the number of publications on these materials, in particular those prepared from hot melts, is very limited. Mostly,

adhesives based on thermo-cured epoxy and MWCNTs have been described in literature ²²⁻²³. In the case of thermoplastic HMAs with CNTs, poly(urethane)s ¹⁷ and poly(olefin)es ¹⁸ based systems have been investigated.

HMAs are not typical homo-polymers but are random polymer blends having low melting points and good adhesive properties ¹⁹. Therefore, they should be considered separately from common composites of homo-polymers and MWCNTs as the effect of MWCNTs on their properties are different ²⁰. They are used in the textile industry to produce non-wovens for surface finishing and inter-leaf materials in carbon fibre reinforced polymers (CFRP), for instance for the aeronautical sector ²¹. It has been shown that thermoplastic fabrics and fibres made of neat HMAs can improve the fracture toughness of CFRP ³⁰⁻³¹. Beyond improvements in mechanical properties, there is also the possibility to enhance the electrical properties of CFRP, currently a topical research area. Hence, the formation of fabrics or fibres made of HMAs doped with CNTs is industrially attractive ²². For this application, we selected commercially available hot melt co-polyamides (coPAs) designed for use in the manufacturing of fibrous materials which could be applied as reinforcement for CFRP.

In this paper, we describe, for the first time, the rheological behaviour and electrical properties of two types of hot melt coPAs mixed with MWCNTs. A masterbatch route was selected for coPA-MWCNT composite production. A critical examination of the rheological and electrical properties of the composites and their relationship with morphology and indirectly, the resultant impact on adhesive properties is presented.

2. Experimental section

2.1. Materials

Two commercial hot melt coPAs, trade names Griltex®D1330A (coPA_A) and Griltex®2A (coPA_B) having different melt viscosities and produced by EMS Griltech, Switzerland were used in this study. The multi-walled carbon nanotubes used (MWCNTs, NC 7000, Nanocyl, Belgium) were produced by catalytic carbon vapour deposition with purity >95% and average diameter (d) of 9.5 nm and length of 1.5 μm . A 7wt% MWCNT masterbatch of both coPA was supplied as pellets by Nanocyl and diluted to concentrations of 1, 2, 3, 4, 5 and 6 wt% MWCNTs. This was achieved using a conical twin screw co-rotating mini-extruder (HAAKE MiniLab, Thermo Scientific) having a bypass cycle which permits the mixing of components for a defined mixing time. The influence of temperature and screw velocity is not in the scope of this paper therefore, all materials were processed using the same conditions. The processing temperature was in the range 160-170 °C, the screw velocity was set to 80 rpm and a total mixing time fixed at 7 mins. Samples for further testing and characterisation were prepared using a HAAKE MiniJet injection moulding machine (Thermo Scientific, Germany). Successful mouldings were achieved using a barrel temperature of 210 °C, a mould temperature of 50 °C, a first pressure of 500 bar and a post-injection pressure of 400 bar. The masterbatch and neat coPAs were dried at 80 °C for 12 h prior to being compounded with the MWCNTs.

2.2. Material and Composite Characterisation

Solution NMR samples were prepared at 20 wt% in a solvent mixture of 2,2,2-trifluoroethanol (TFE) and CDCl_3 (80:20 respectively), according to the procedure

of Davis *et al.*¹ ¹H NMR spectra were recorded on a Bruker DPX-400 spectrometer operating at a frequency of 400.05 MHz and ¹³C NMR spectra were recorded on the same instrument at 100.59 MHz (512 scans, 4 s relaxation time, 298.2 K).

The distribution and the dispersion of the MWCNTs in the composites were analysed by light microscopy and Transmission Electron Microscopy (HR STEM Hitachi S5500) at a voltage of 30kV. Thin slices of each composite material of 80-90nm thickness were micro-tomed (UM6 ultra-microtome, Leica Mirosystem Germany) from injection moulded samples in the injection direction. The cutting process was performed with diamond knives at a temperature of 100 °C with a cutting speed of 1 mm/s. The optical micrographs of the 1 wt% and 7 wt% MWCNT-filled co-polyamides were analysed using image software (ImageJ) in order to assess the macro-state of MWCNT dispersion. Agglomerates with an area below 1µm were rejected from the analysis, as classically inclusions greater than 1µm act as stress concentration points in polymers. The mean diameter of the MWCNT agglomerates was calculated from multiple images.

Rheology measurements were performed on a MARS III oscillatory rheometer (Thermo Scientific, Germany) using a parallel plate geometry (gap width=2 mm) at 200 °C. Firstly, the amplitude sweep test was carried out to find the linear elastic range for neat and MWCNT filled co-polyamides. The upper value of strain amplitude just prior to the reduction in moduli was chosen for the stress-controlled rotational measurements. The rheological measurements of all materials were conducted for a frequency sweep between 0.1-100 rad/s.

Dielectric spectra were recorded at room temperature (RT). The complex dielectric permittivity, ϵ^* was measured with a LCR HP4284A meter (Keysight Technologies, USA) and, the equivalent electrical circuit was selected as the capacitance and the tangent

of losses connected in parallel. From these quantities, according to the planar capacitor formula, the complex dielectric permittivity was calculated. Silver paste was used to minimise contact resistance. The amplitude of the AC electric field was selected as 1V, a meaningful voltage typically used to assess electrical conductivity in bulk samples. It gives the best signal to noise ratio in comparison with lower voltage values and avoids non-linear dielectric effects, which were observed at higher voltages (the typical thickness of the sample was 1 mm)²³. The electrical conductivity, σ was calculated according to equation $\sigma=2\pi v\epsilon_0\epsilon^*$, where $\omega=2\pi v$ and v is the measurement frequency.

Thermal properties of neat coPAs and their composites were examined using DSC (Q-1000 (TA Instruments, USA). 9mg of each material was placed in an aluminium hermetic crucible and then the heat-cool-heat program was applied in a nitrogen atmosphere and with a scan rate 10°C/min. The crystalline content was not calculated as this is not directly possible as there is a contribution to the melting endotherms from more than one Nylon. The value for a theoretically 100% crystalline coPA_A or coPA_B required to determine crystalline content is not known. Therefore, the enthalpy of fusion measured which is directly related to the overall crystalline content, was used to study the effect of MWCNTs on the crystal phase in coPAs.

Contact angle measurements were made on injection molded bars using a goniometer DataPhysic OCA 15EC (DataPhysics Instruments GmbH, Germany) equipped with a camera. Contact angles were measured at a minimum of five places on each sample and then the average value calculated. The measurements were performed using water as a liquid at RT. From left and right measured contact angles of a droplet the software calculated the average surface energy using an equation of a state.

3. Results and discussion

In the first instance, we attempted to study and understand the co-polymer composition of the two proprietary coPAs used in this study. Neat coPA_A and coPA_B were prepared for NMR analysis and subsequently analysed using the procedure outlined by Davis *et al.* for characterization of unknown poly(amide) homo-polymers and co-polymers²⁴. Unfortunately, the ¹³C NMR data obtained included multiple peaks in the aliphatic region which do not correspond to those described in the Davis procedure nor could be identified from the published literature. However, the data does permit an estimation of some of the co-monomers used to create these co-polymers. It is important to know co-polymer composition as addition of MWCNTs to Nylons is known to have a strong nucleating effect on the polymer, alter crystallisation kinetics and content and potentially alter the adhesive properties of the coPAs²²⁻²³. Based on the ¹³C NMR data, and focusing in particular on the aliphatic region (see Figure 1) coPA_A was found to contain trans-Nylon 6 and at least one other type of Nylon that is not Nylon 6; 6,6; 6,9; 6,10; 6,12; 11; 12 or caprolactam. There are also no peaks in the aromatic region of the ¹H NMR data obtained for coPA_A.

The ¹³C NMR spectrum for coPA_B differed markedly from that for coPA_A (see Figure 2). It is clear from the data that this sample contains trans-Nylon 6 and also trans-Nylon 6,6 as well as the same unknown Nylon identified in coPA_A. There are also peaks in the spectrum consistent with at least one other species which may or may not be a poly(amide) and is certainly not Nylon 6; 6,6; 6,9; 6,10; 6,12; 11; 12 or caprolactam. These could be associated with plasticizers, waxes and others resins present in the blend, detail not made readily available by the resin producer.

The extent of MWCNT dispersion and distribution in the hot melt coPAs was investigated using light optical and HRTEM microscopy, see Figures 3, 4 and 5. By way of example, the images and analysis for composites of 7 wt% and 1 wt% MWCNTs filled coPAs are presented. Ideally, the MWCNT agglomerates should be broken up by erosion and/or rupture ⁶. However, this is difficult to achieve and the physical properties of polymer and mixing technique employed play a major role in achieving effective MWCNTs dispersion ¹¹. Here, extrusion was utilised and even with the application of relatively high shear forces the MWCNTs at the highest loading (7 wt%) were not well dispersed in both polymer matrices, see Figure 3 a and b. MWCNT agglomerates of different sizes, some as large as 60µm were observed, those in coPA_B were generally larger than those observed in coPA_A. At lower MWCNTs loadings, e.g. 1 wt%, see Figure 3 c and d, the macro-dispersion in coPA_A and coPA_B was much better. Significantly, fewer of the large MWCNT agglomerates were observed. At this length scale it is not possible to confirm in which coPA the MWCNT dispersion is best. It is now well established that mixing of MWCNTs into polymers via melt mixing results in incomplete breakage of MWCNT agglomerates however, from Figure 3 c and d the MWCNT dispersion and distribution in both co-polyamides is relatively homogenous with much fewer agglomerates ⁶.

The distribution of MWCNT agglomerate size in both coPAs was assessed using image analysis of the optical photographs obtained. Exhaustive inspection and analysis of multiple images was performed and histograms generated showing the relationship between the number of agglomerates and mean agglomerate diameter in µm, see Figure 4. It is clear for both coPAs that at high MWCNT loading (7wt%) a broad distribution of agglomerate sizes are observed with maximum diameter up to 50µm, for

less viscous coPA_B. After dilution to 1wt% MWCNTs, for coPA_A, the maximum MWCNT agglomerate size was around 10 μ m. For the composite of coPA_B and 1 wt% MWCNTs, the maximum mean MWCNT agglomerate was slightly larger, typically 15 μ m. These observations reflect the fact that during the second extrusion step the MWCNT agglomerates are destroyed leading to better dispersion and distribution of MWCNT in polymer melts. It has been observed, that dilution of a 15 wt% MWCNT polypropylene masterbatch by twin screw extrusion results in better MWCNT dispersion and distribution in the PP matrix²⁵. For the composites described here, melt viscosity also plays a role in determining the extent of MWCNT dispersion, as the coPA_A has a higher viscosity than coPA_B which contributes to higher shear forces acting on and breaking the MWCNT agglomerates into smaller sizes²⁶.

Further assessment of the extent of MWCNT dispersion in both coPAs matrices was investigated using HRTEM imaging. Figure 5 shows the level of MWCNT dispersion in both coPA masterbatches, i.e. with 7 wt% MWCNTs. At this magnification, the MWCNTs are highly dispersed and agglomerates not observed. The MWCNTs, as expected are, more densely packed at higher loadings. Similar states of dispersion were obtained when a 15 wt% MWCNT-polycarbonate masterbatch was diluted to 1 wt% MWCNTs using a similar melt mixing method employed in this work²⁷. From Figure 5 c) and d), there is strong evidence to suggest the MWCNTs are oriented in the direction of material flow during injection molding. This can lead to a lower probability of CNT-CNT interaction and resulting in little or no change in electrical conductivity of the matrix polymer²⁶.

The extent of MWCNT dispersion was also studied by examining the rheological behaviour of the hot melt coPA composites from oscillatory rheology measurements on

injection molded samples. It is well known that when CNTs are well dispersed and form an inter-connected network in a polymer matrix the composite material behaves responds more like a solid^{34,35}. Figures 6 and 7 show the variation in storage modulus (G'), loss modulus (G'') and complex viscosity (η^*) as a function of frequency for coPA_A and coPA_B and composites of both with up to 7 wt% MWCNTs, respectively. At low frequencies and, for both coPAs systems, the viscosity increased by 4 to 5 orders of magnitude on MWCNT addition, confirming the formation of a percolated network of MWCNTs¹⁴. The unfilled coPAs behave as non-Newtonian liquids as their viscosity is not dependent on frequency over the range examined. The viscosity curve for the composite of coPA_A and 1 wt% MWCNTs is almost independent of frequency, similar to that for neat coPA_A. In contrast, for the composite of coPA_B and 1 wt% MWCNTs a ten-fold increase in η^* was observed relative to neat coPA_B. Further addition of MWCNTs to both coPAs resulted in an increase in η^* . This suggests that a rheological percolation threshold between 1 wt% and 2 wt% MWCNTs when added to coPA_A and between 0 and 1 wt% MWCNTs when added to coPA_B. These values are similar to those for hot melt poly(olefin)s filled with 2.5 wt% MWCNTs (also NC 7000, Nanocyl) reported by Pötschke *et al.* in which a rheological percolation threshold was recorded at 0.75 wt% MWCNTs²⁹. The difference in the melt viscosity of coPA_B and coPA_A, the former about two times lower than the latter may allow the MWCNTs to be more easily mixed in the polymer matrix achieving rheological percolation at lower MWCNT content. The influence of polymer melt viscosity on MWCNT dispersion and distribution and thus electrical conductivity has been reported for common thermoplastic polymers¹⁰ and, will be discussed further below.

The large increase in complex viscosity of both coPAs on MWCNT addition was concomitant with a significant increase in storage modulus (G')³⁰, by 5 orders of magnitude. From figures 6 and 7, the higher the MWCNT loading the higher G' within the whole frequency range examined for both types of hot melt coPAs. The variation in G' as a function of frequency maps that seen with η^* , further evidence for rheological percolation between 1 wt% and 2 wt % MWCNTs for coPA_A and below 1 wt% MWCNTs for coPA_B. For PU based HMA, the rheological percolation threshold was found between 2 to 4 wt% MWCNTs at 100 °C¹⁷. In turn for higher MWCNT content the differences between the G' curves are smaller because the network of nanotubes which has already been created disturbs less the motion of the polymer chains under shear³¹. When the values of G' and G'' are compared, it can be found that for both coPAs G'' is higher than G' , the inverse to that obtained for the nanocomposites, i.e. G'' is lower than G' . The elastic behaviour (expressed by G') predominates the viscous one, behaviour regularly observed for other CNT filled thermoplastic polymers, for instance polypropylene³², polystyrene³³, poly(methyl methacrylate)³⁴ and polycarbonate³⁵ and the composites respond more like a solid. Although the oscillatory rheology measurements were performed at 200 °C, the significant increase in melt viscosity obtained for both coPAs on addition of MWCNTs may impact the application of these adhesives to other materials.

Further confirmation of rheological percolation was determined from examining Cole-Cole plots, i.e. the logarithmic dependence between G' versus G'' , see Figures 6 c) and 7 c). It can be seen that with increasing G'' , G' increased. A deviation from a linear relationship between G'' and G' is characteristic of the onset of percolation on addition of MWCNTs³⁰. After addition of the MWCNTs the curves deviated from the curve for the

neat unfilled coPAs. However, in the case of coPA_A the curve deviate at some MWCNT loading between 2 wt% and 3 wt% MWCNTs (i.e. percolation is attained at some loading between 2 wt% and 3wt% MWCNT inclusion). However, for coPA_B deviation was obvious below 1 wt% MWCNT addition. This might be expected given the melt viscosity of coPA_B is about 10 times less than coPA_A. For both systems, addition of relatively low MWCNT loading hinders polymer chain dynamics.

The frequency dependence of dielectric permittivity and electrical conductivity (AC) for composites of coPA_A hot melt and MWCNTs is shown in Figure 8. The dielectric permittivity and the electrical conductivity of pure coPA_A matrix is quite low (less as 8 and 10^{-8} S/m, respectively, at 129 Hz frequency), as expected. For the composites of coPA_A and 1 wt% MWCNT inclusions the dielectric and electric properties are similar to the unfilled matrix properties, no frequency independent (DC) conductivity was observed at low frequencies. In contrast, for composites with addition of 3 wt% MWCNTs to coPA_A, at low frequencies the frequency independent plateau was observed and values for dielectric permittivity are high (higher than 10^3). Hence, we assume that the electrical percolation threshold is close to 3 wt% MWCNTs for coPA_A hot melt based composites. By coincidence, this is a similar MWCNT loading at which rheological percolation was obtained for these composites.

The frequency dependence of dielectric permittivity and electrical conductivity for the coPA_B hot melt and composites with MWCNTs is shown in Figure 9. For these samples, the DC conductivity plateau was observed for the composites with 1 wt% MWCNT addition, therefore the percolation threshold is close (however below) 1 wt% MWCNTs. This suggests the composites based on coPA_B have a lower electrical percolation

threshold than the coPA_A based composites. In comparison, an electrical percolation threshold at 0.75 wt% MWCNTs has been reported for HMA based on poly(olefin)s¹⁸.

The electrical percolation threshold can be obtained from the MWCNT concentration dependence of dielectric permittivity and electrical conductivity at a fixed frequency (129 Hz), see Figure 10. Indeed, a clear step jump was observed close to the percolation threshold in the concentration dependence of the dielectric permittivity and the electrical conductivity. According to the excluded volume theory electrical percolation is inversely proportional to the diameter/length (aspect ratio) of CNTs³⁶. However, usually composites comprise individual, perfectly dispersed MWCNTs as well as MWCNTs agglomerates.

The percolation threshold of these composites can be estimated from equation 1;

$$f_c = v\phi\pi + (1 - v)27\pi/4p^2 \quad (1)$$

where ϕ is the localized volume content of MWCNTs in an agglomerate, and v is the volume fraction of agglomerated MWCNTs³⁷. Therefore, the difference of the percolation threshold values in the composites with the different coPAs can be explained by the different levels of MWCNT dispersion and distribution in both polymer matrices.

In our study, the values for electrical percolation threshold are slightly higher than those for rheological percolation. The differences in the electrical properties can be related not only to MWCNT agglomerate size and dispersion but to the changes in the coPA crystalline content after MWCNT addition. Generally, it should be noted that addition of CNTs can alter crystallization kinetics and the crystalline content of polymers, including polyamides^{38,39,40,41,42,43}.

Thus, the effect of MWCNT addition on the thermal properties of both coPAs and composites were investigated using DSC, see Figures 11, 12 and 13. A heating/cooling

regime of heat-cool-reheat was adopted to remove the thermal history from the samples as a consequence of melt mixing process and, the various thermal properties were determined from the resulting thermograms and their values listed in Table 2. Examination of both sets of samples post processing (i.e. first heating), revealed interesting behaviour. For both coPA_A and coPA_B two processes were obtained, see Figure 11. Firstly, a glass transition (T_g) at about 46 °C for coPA_A, typical of the T_g of Nylon 6 and, a melting endotherm (T_m) with a peak maximum at 123 °C were observed. On addition of MWCNTs up to a loading of 6 wt%, the T_g process became more rounded resembling that of a gel and increasing in temperature by about 10 °C up to 55 °C. Interestingly, when the MWCNT loading was increased further to 7 wt%, this low temperature process was resolved in to two T_g 's the first centered at about 51 °C, the second at 75 °C, perhaps associated with Nylon 6 and Nylon 6,6, for coPA_B but associated with Nylon 6 and another unassigned Nylon for coPA_A. The T_m maxima increased by around 8°C, but the enthalpy associated each decreased with increasing MWCNT inclusion, from 66 J/g for unfilled coPA_A down to 32 J/g for the composite with 7 wt% MWCNTs, i.e. the crystalline content decreased by just over half. For coPA_B, a clear T_g was obtained at about 70 °C, typical of Nylon 6,6 and again a melting endotherm, but with a slightly lower T_m (121 °C) compared with coPA_A (129 °C). There is also some evidence for a second T_g at about 46 °C and clear evidence for cold crystallization for coPA-B with a process centered at 95 °C. On addition of MWCNTs up to 6 wt%, it appears that perhaps a single broad process could be two T_g 's overlapped which are then resolved when 7 wt% MWCNTs were added into two single T_g 's, one at about 53 °C, the other at about 82 °C.

The DSC traces of the samples obtained upon cooling showed different features. In the temperature range examined, no thermal processes were seen for unfilled coPA_A, see Figure 12 b). However, for the composites of coPA_A with MWCNTs, a very broad process was observed, typically with an onset temperature at about 80 °C extending up to 120 °C, but with maxima which increased with increasing MWCNT loading, reflecting the heterogeneous nucleating effect of MWCNTs for the crystalline fraction of coPA_A. Similarly, for unfilled coPA_B, no features were observed in the DSC trace upon cooling, see Figure 13 b). Addition of MWCNTs to coPA_B also resulted in nucleating this copolyamide however, a sharper exotherm centred at about 84 °C was obtained compared with that for coPA_A. Upon 2 wt% or greater MWCNT inclusions the evolution of a second exotherm at higher temperatures (~95 °C), initially as a shoulder, was obtained. Unlike for coPA_A where an increase in crystalline content was obtained on MWCNT addition, the crystalline content of the coPA_B composites, allowing for instrument error was similar. Clearly, the MWCNTs are nucleating these coPAs, but more so coPA_B. The splitting of the exotherms has previously been assigned to morphological modifications as opposed to a second crystal polymorph³⁹.

The DSC traces for the second heating cycle (see Figures 12 a) and 13 a)) for both sets of composites, displayed a broad (from 110 °C to 150 °C) single transition for the coPA_A systems centered at about 132 °C but a much sharper (115 °C to 135 °C) endotherm for the coPA_B systems, with a maximum at about 126 °C. However, for the coPA_B composites a second broad process (85 °C to 105 °C) was also observed. The breadth of the temperature ranges for these endothermic processes for both sets of composites and any effects MWCNT addition has on them is important with regard the application of these HMAs in practice.

The results presented clearly showed that addition of MWCNTs to coPA_A and coPA_B altered the thermal and rheological properties of these coPAs. We also showed a random dispersion and distribution of the MWCNTs in both polymer matrices. Intuitively, it would then be expected that the MWCNT inclusions would also affect the surface properties of these coPAs and *de facto* their adhesive properties. Contact angle measurements were performed on all samples and the respective surface energies calculated, both are listed in Table 3. Indirectly, these parameters can be used to assess the effect of MWCNT addition on the adhesiveness of both coPAs. Firstly, it is clear that the surface energy of coPA_B is much less than that for coPA_A, presumably a consequence of the differences in the co-polymer composition of each. Second, the addition of MWCNTs to coPA_A resulted in a modest change in contact angle and surface energy. In contrast, addition of MWCNTs to coPA_B gave a significant decrease in contact angle and increase in surface energy. Indeed, the inclusion of 2 wt% MWCNTs to coPA_B gave very similar contact angle and surface energy values to unfilled coPA_A and its composites with MWCNTs, see Table 3. Addition of MWCNTs renders the surface of coPA_B more hydrophilic and the increase in surface energy obtained is a measure of increased attractive forces, which promotes adhesion. Thus, the wettability of coPA_B has been significantly altered by MWCNT addition, see Figure 14, and the increase in wettability and surface energy implies the adhesive properties of coPA_B have been improved to a level comparable to unfilled coPA_A with even 2 wt% MWCNT inclusion.

Conclusions

Two types of hot melt coPA filled with 7 wt% MWCNTs and then diluted to lower MWCNT loadings were prepared using a twin-screw extruder. Incorporation of higher MWCNT loadings into both coPAs resulted in smaller agglomerate sizes, although agglomerates having diameters up to 35 μ m in coPA_A and 50 μ m in coPA_B were observed. Interestingly, dilution of both masterbatches to 1 wt% resulted in a larger number of smaller agglomerates with diameters typically below 20 μ m but some up to 70 μ m, the latter related to re-agglomeration of MWCNTs during the dilution step. Rheological percolation was found between 1 wt% and 2 wt% and below 1 wt% MWCNTs for coPA_A and coPA_B, respectively, as the mobility of polymer chains are greater for the less viscous coPA_B. Unsurprisingly, electrical percolation was achieved at approximately 1 wt% MWCNTs in coPA_B while for coPA_A at about 3 wt% MWCNTs. The differences in electrical properties between the MWCNT filled coPAs are related to both the level of MWCNT dispersion and distribution but also to changes in the crystalline phase of both coPAs due to MWCNT addition. Thermal analysis confirmed that the MWCNTs act as heterogeneous nucleating agents leading to a slight increase in crystalline phase content for coPA_A. Most importantly, the adhesive properties of both coPAs as extracted from contact angle measurements and surface energy calculations showed that addition of MWCNTs significantly altered the adhesive properties of coPA_B.

References

1. Sathyanarayana S, Hübner C. Thermoplastic Nanocomposites with Carbon Nanotubes. In: J. Njuguna, ed. *Structural Nanocomposites*. Springer-Verlag Berlin Heidelberg; 2013:19-61. doi:10.1007/978-3-642-40322-4.
2. So HH, Cho JW, Sahoo NG. Effect of carbon nanotubes on mechanical and electrical properties of polyimide/carbon nanotubes nanocomposites. *Eur Polym J*. 2007;43(9):3750-3756. doi:10.1016/j.eurpolymj.2007.06.025.
3. Warriar A, Godara A, Rochez O, et al. The effect of adding carbon nanotubes to glass/epoxy composites in the fibre sizing and/or the matrix. *Compos Part A Appl Sci Manuf*. 2010;41(4):532-538. doi:10.1016/j.compositesa.2010.01.001.
4. Matzeu G, Pucci a., Savi S, Romanelli M, Di Francesco F. A temperature sensor based on a MWCNT/SEBS nanocomposite. *Sensors Actuators, A Phys*. 2012;178:94-99. doi:10.1016/j.sna.2012.02.043.
5. Yin C, Dong J, Li Z, Zhang Z, Zhang Q. Composites : Part B Large-scale fabrication of polyimide fibers containing functionalized multiwalled carbon nanotubes via wet spinning. *Compos PART B*. 2014;58:430-437. doi:10.1016/j.compositesb.2013.10.074.
6. Kasaliwal GR, Pegel S, Göldel A, Pötschke Petra P, Heinrich G. Analysis of agglomerate dispersion mechanisms of multiwalled carbon nanotubes during melt mixing in polycarbonate. *Polymer (Guildf)*. 2010;51(12):2708-2720. doi:10.1016/j.polymer.2010.02.048.
7. Alig I, Pötschke P, Lellinger D, et al. Establishment, morphology and properties

- of carbon nanotube networks in polymer melts. *Polymer (Guildf)*. 2012;53(1):4-28. doi:10.1016/j.polymer.2011.10.063.
8. Prashantha K, Soulestin J, Lacrampe MF, Claes M, Dupin G, Krawczak P. Multi-walled carbon nanotube filled polypropylene nanocomposites based on masterbatch route: Improvement of dispersion and mechanical properties through PP-g-MA addition. *Express Polym Lett*. 2008;2(10):735-745. doi:10.3144/expresspolymlett.2008.87.
 9. Harper S, Wohlleben W, Doa M, et al. Measuring Nanomaterial Release from Carbon Nanotube Composites: Review of the State of the Science. *J Phys Conf Ser*. 2015;617:12026. doi:10.1088/1742-6596/617/1/012026.
 10. Socher R, Krause B, Müller MT, Boldt R, Pötschke P. The influence of matrix viscosity on MWCNT dispersion and electrical properties in different thermoplastic nanocomposites. *Polymer (Guildf)*. 2012;53(2):495-504. doi:10.1016/j.polymer.2011.12.019.
 11. Kasaliwal GR, Villmow T, Pegel S, Pötschke P. Influence of material and processing parameters on carbon nanotube dispersion in polymer melts. In: McNally T, Pötschke P, eds. *Polymer–Carbon Nanotube Composites. Preparation, Properties and Applications*. Woodhead Publishing Limited; 2011:92-132. doi:10.1533/9780857091390.1.92.
 12. McClory C, Pötschke P, McNally T. Influence of screw speed on electrical and rheological percolation of melt-mixed high-impact polystyrene/MWCNT nanocomposites. *Macromol Mater Eng*. 2011;296(1):59-69. doi:10.1002/mame.201000220.

13. Sahoo NG, Rana S, Cho JW, Li L, Chan SH. Polymer nanocomposites based on functionalized carbon nanotubes. *Prog Polym Sci.* 2010;35(7):837-867. doi:DOI 10.1016/j.progpolymsci.2010.03.002.
14. Mohammad M, Winey KI. Polymer Nanocomposites Containing Carbon Nanotubes. *Macromolecules.* 2006;39(16):5194-5205. doi:10.1021/ma060733p.
15. Bauhofer W, Kovacs JZ. A review and analysis of electrical percolation in carbon nanotube polymer composites. *Compos Sci Technol.* 2009;69(10):1486-1498. doi:10.1016/j.compscitech.2008.06.018.
16. Nuzhnyy D, Savinov M, Bovtun V, et al. Broad-band conductivity and dielectric spectroscopy of composites of multiwalled carbon nanotubes and poly(ethylene terephthalate) around their low percolation threshold. *Nanotechnology.* 2013;24:55707. doi:10.1088/0957-4484/24/5/055707.
17. Fernández M, Landa M, Muñoz ME, Santamaría A. Thermal and Viscoelastic Features of New Nanocomposites Based on a Hot-Melt Adhesive Polyurethane and Multi-Walled Carbon Nanotubes. *Macromol Mater Eng.* 2010;295(11):1031-1041. doi:10.1002/mame.201000176.
18. Franziska Wehnert, Pötschke P, Jansen I. Hotmelts with improved properties by integration of carbon nanotubes. *Int J Adhes Adhes.* 2015;62:63-68. doi:10.1016/j.ijadhadh.2015.06.014.
19. Brewis D. Hot melt adhesives. In: *Handbook of Adhesion.* Elsevier B.V.; 2005:711-757. doi:10.1016/B978-0-444-51140-9.50015-9.
20. Ebnesajjad S. Characteristics of adhesive materials. In: Sina Ebnesajjad, ed.

- Handbook of Adhesives and Surface Preparation*. Elsevier Inc.; 2011:137-183.
doi:10.1016/B978-1-4377-4461-3.10008-2.
21. da Costa AP, Botelho EC, Costa ML, Narita NE, Tarpani JR. A review of welding technologies for thermoplastic composites in aerospace applications. *J Aerosp Technol Manag*. 2012;4(3):255-265. doi:10.5028/jatm.2012.04033912.
 22. Friedrich K, Breuer U. *Multifunctionality of Polymer Composites: Challenges and New Solutions*. Elsevier Science; 2015.
https://books.google.com/books?id=L_qcBAAAQBAJ&pgis=1. Accessed January 21, 2016.
 23. Liu L, Kong LB, Matitsine S, Liu L, Kong LB, Matitsine S. Tunable effective permittivity of carbon nanotube composites Tunable effective permittivity of carbon nanotube composites. 2010;113106(2008):1-4. doi:10.1063/1.2983745.
 24. Davis RD, Jarrett WL, Mathias LJ. Solution ¹³C NMR spectroscopy of polyamide homopolymers commercial copolymers. *Polymer (Guildf)*. 2001;42:2621-2626.
 25. Prashantha K, Soulestin J, Lacrampe MF, Krawczak P, Dupin G, Claes M. Masterbatch-based multi-walled carbon nanotube filled polypropylene nanocomposites : Assessment of rheological and mechanical properties. *Compos Sci Technol*. 2009;69(11-12):1756-1763. doi:10.1016/j.compscitech.2008.10.005.
 26. Mahmoodi M, Arjmand M, Sundararaj U, Park S. The electrical conductivity and electromagnetic interference shielding of injection molded multi-walled carbon nanotube/polystyrene composites. *Carbon N Y*. 2012;50(4):1455-1464.

doi:10.1016/j.carbon.2011.11.004.

27. Pötschke P, Bhattacharyya AR, Janke A. Melt mixing of polycarbonate with multiwalled carbon nanotubes: Microscopic studies on the state of dispersion. *Eur Polym J*. 2004;40(1):137-148. doi:10.1016/j.eurpolymj.2003.08.008.
28. Handge U a., Pötschke P. Deformation and orientation during shear and elongation of a polycarbonate/carbon nanotubes composite in the melt. *Rheol Acta*. 2007;46:889-898. doi:10.1007/s00397-007-0179-6.
29. Pötschke P, Jansen I. Hotmelts with improved properties by integration of carbon nanotubes. *Int J Adhes Adhes*. 2015;62(JUNE):63-68. doi:10.1016/j.ijadhadh.2015.06.014.
30. Nobile MR. Rheology of polymer–carbon nanotube composites melts. *Polym Nanotub Compos Prep Prop Appl*. 2011:428-481. doi:10.1533/9780857091390.2.428.
31. Bae WS, Kwon OJ, Kim BC, Chae DW. Effects of multi-walled carbon nanotubes on rheological and physical properties of polyamide-based thermoplastic elastomers. *Korea Aust Rheol J*. 2012;24(3):221-227. doi:10.1007/s13367-012-0027-9.
32. Seo MK, Park SJ. Electrical resistivity and rheological behaviors of carbon nanotubes-filled polypropylene composites. *Chem Phys Lett*. 2004;395(1-3):44-48. doi:10.1016/j.cplett.2004.07.047.
33. Kota AK, Cipriano BH, Duesterberg MK, et al. Electrical and Rheological Percolation in Polystyrene / MWCNT Nanocomposites. *Macromolecules*.

- 2007;40:7400-7406. doi:10.1021/ma0711792.
34. Du F, Scogna RC, Zhou W, Brand S, Fischer JE, Winey KI. Nanotube networks in polymer nanocomposites: Rheology and electrical conductivity. *Macromolecules*. 2004;37(24):9048-9055. doi:10.1021/ma049164g.
 35. Dijkstra DJ, Cirstea M, Nakamura N. The orientational behavior of multiwall carbon nanotubes in polycarbonate in simple shear flow. *Rheol Acta*. 2010;49(7):769-780. doi:10.1007/s00397-010-0457-6.
 36. Deng H, Lin L, Ji M, Zhang S, Yang M, Fu Q. Progress on the morphological control of conductive network in conductive polymer composites and the use as electroactive multifunctional materials. *Prog Polym Sci*. 2014;39(4):627-655. doi:10.1016/j.progpolymsci.2013.07.007.
 37. Li J, Ma PC, Chow WS, To CK, Tang BZ, Kim JK. Correlations between percolation threshold, dispersion state, and aspect ratio of carbon nanotubes. *Adv Funct Mater*. 2007;17(16):3207-3215. doi:10.1002/adfm.200700065.
 38. Phang IY, Ma J, Shen L, Liu T, Zhang W-D. Crystallization and melting behavior of multi-walled carbon nanotube-reinforced nylon-6 composites. *Polym Int*. 2006;55(1):71-79. doi:10.1002/pi.1920.
 39. Brosse AC, Tencé-Girault S, Piccione PM, Leibler L. Effect of multi-walled carbon nanotubes on the lamellae morphology of polyamide-6. *Polymer (Guildf)*. 2008;49:4680-4686. doi:10.1016/j.polymer.2008.08.003.
 40. Krause B, Pötschke P, Häußler L. Influence of small scale melt mixing conditions on electrical resistivity of carbon nanotube-polyamide composites.

Compos Sci Technol. 2009;69(10):1505-1515.

doi:10.1016/j.compscitech.2008.07.007.

41. Li J, Fang Z, Tong L, Gu A, Liu F. Effect of multi-walled carbon nanotubes on non-isothermal crystallization kinetics of polyamide 6. *Eur Polym J.* 2006;42(12):3230-3235. doi:10.1016/j.eurpolymj.2006.08.018.
42. Sun L, Yang JT, Lin GY, Zhong MQ. Crystallization and thermal properties of polyamide 6 composites filled with different nanofillers. *Mater Lett.* 2007;61(18):3963-3966. doi:10.1016/j.matlet.2006.12.090.
43. Krause B, Boldt R, Häußler L, Petra Pötschke. Ultralow percolation threshold in polyamide 6.6/MWCNT composites. *Compos Sci Technol.* 2015;114:119-125. doi:10.1016/j.compscitech.2015.03.014.

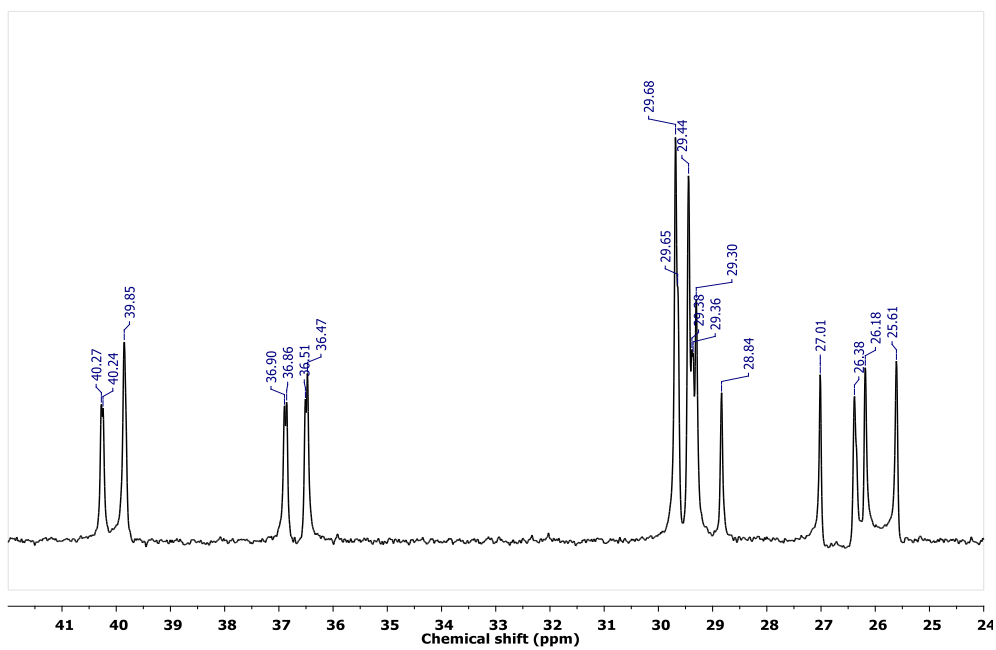


Figure 1: ^{13}C NMR spectrum for coPA_A.

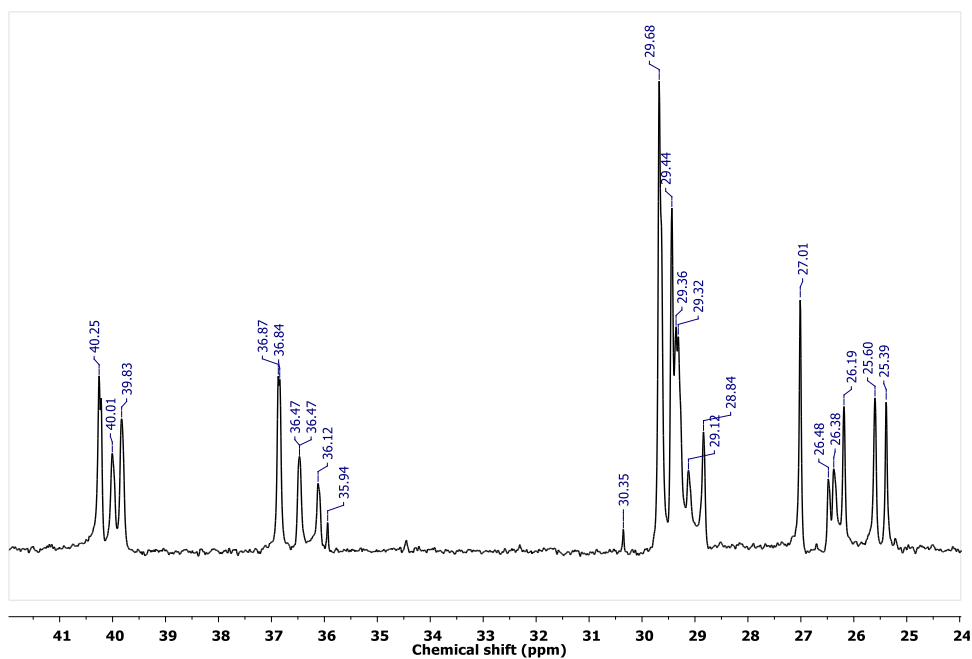


Figure 2: ^{13}C NMR spectrum for coPA_B.

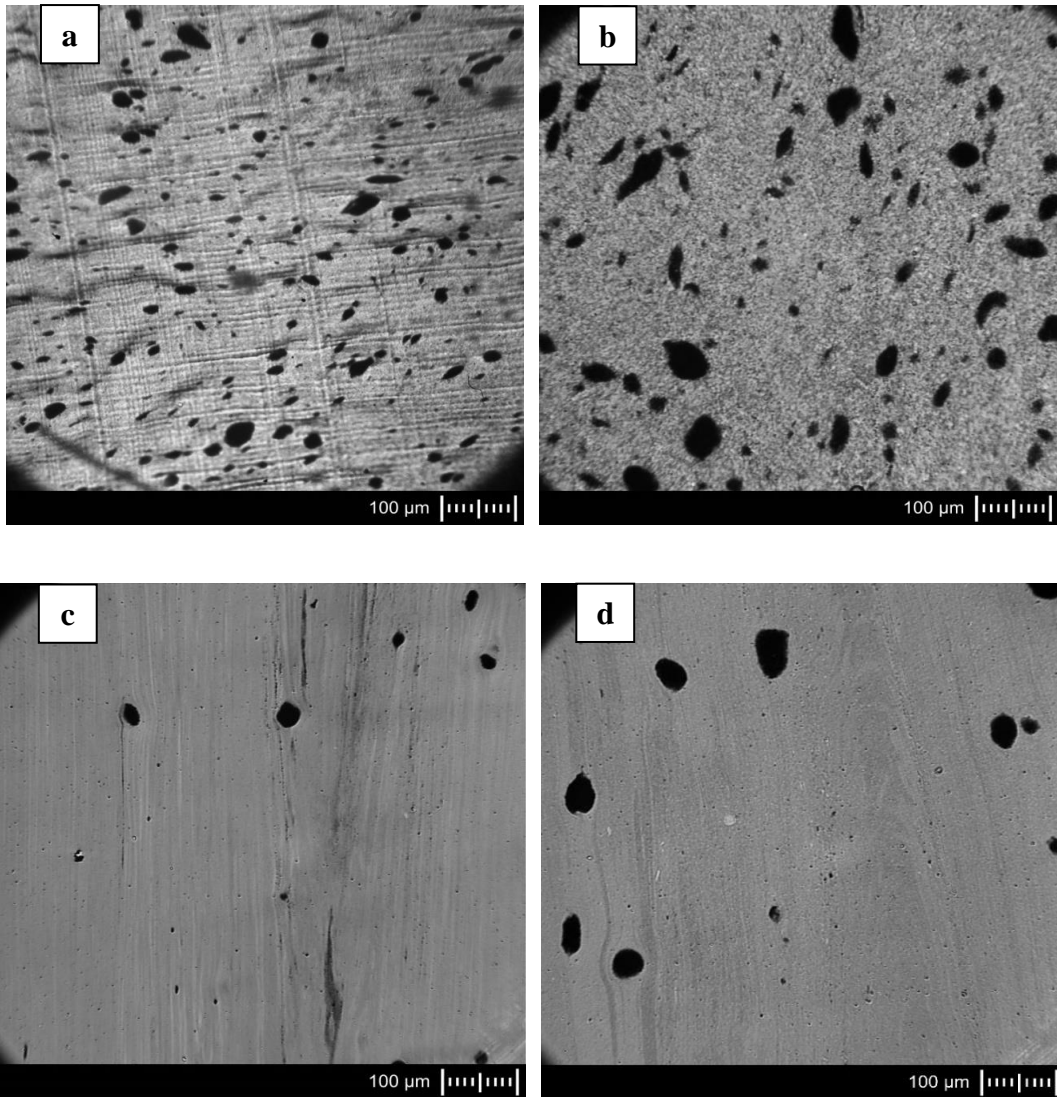


Figure 3: Light microscopy images of composites of a) coPA_A + 7wt% MWCNTs, b) coPA_B + 7wt% MWCNTs, c) coPA_A + 1wt % MWCNTs and d) coPA_B + 1wt% MWCNTs (D).

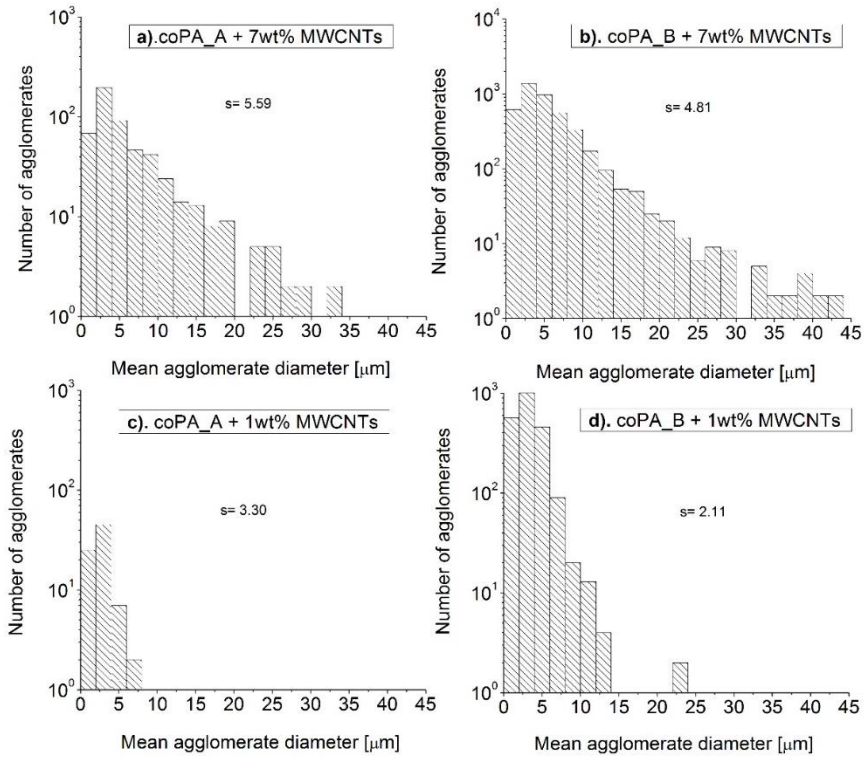


Figure 4: MWCNT agglomerate size distribution of composites of a) coPA_A and b) coPA_B with 7wt% MWCNTs and, c) coPA_A and d) coPA_B with 7wt% MWCTs. (Standard deviations (s) are inset in each figure)

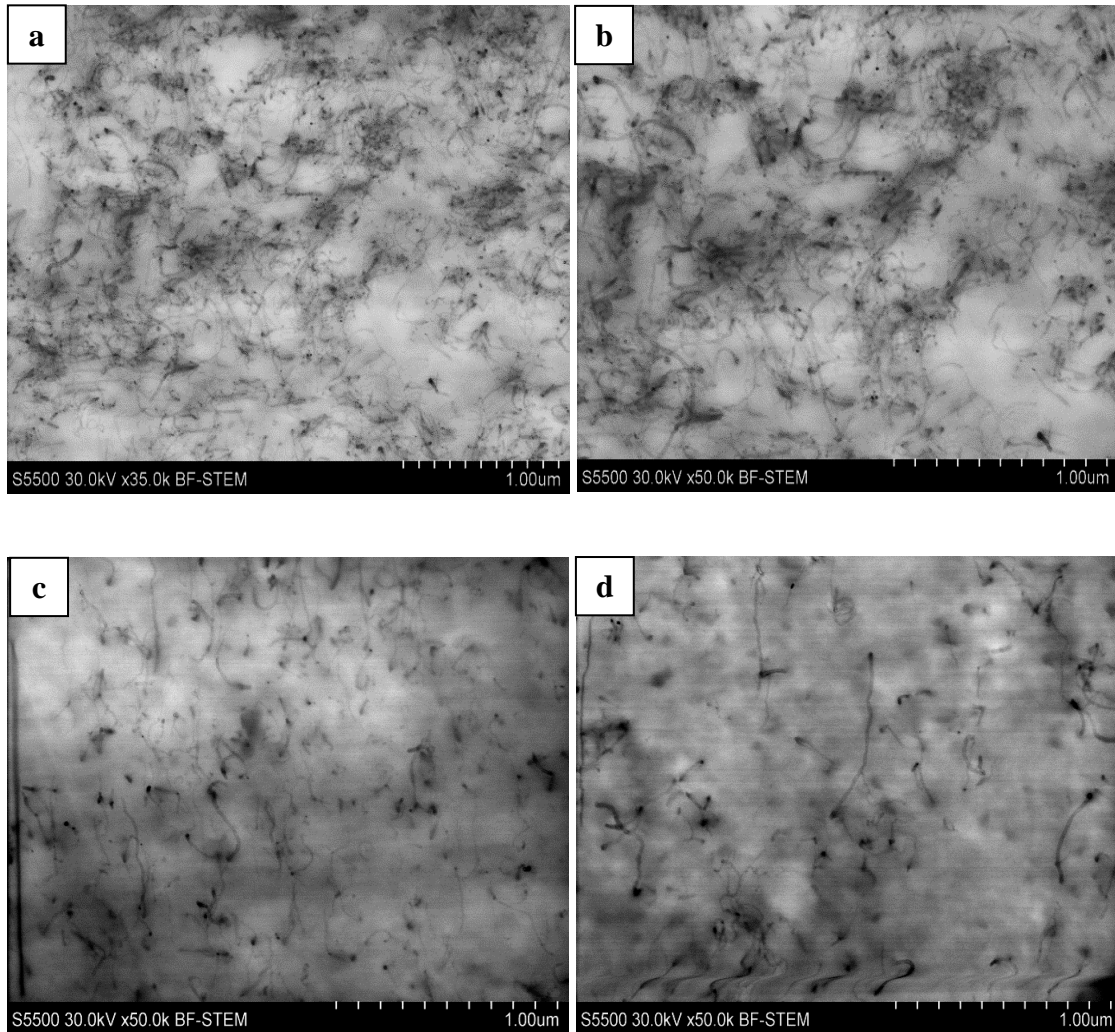


Figure 5: HRTEM micrographs of both masterbatches, a) coPA_A and 7wt% MWCNTs, and b) coPA_B and 7wt% MWCNTs and, images taken from injection moulded samples of c) coPA_A and 1wt% MWCNTs and d) coPA_B and 1wt% MWCNTs.

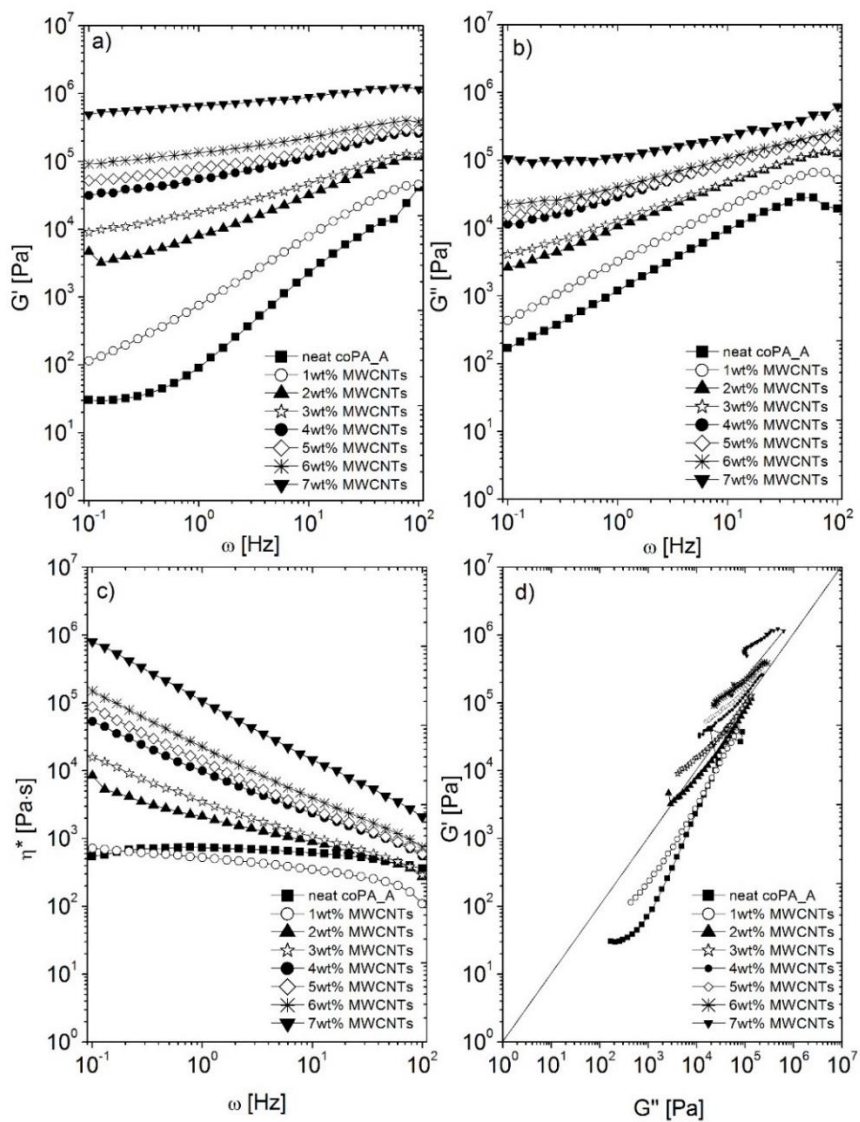


Figure 6: Variation in a) G' , b) G'' and c) complex viscosity (η^*) as a function of frequency and d) Cole-Cole plot.

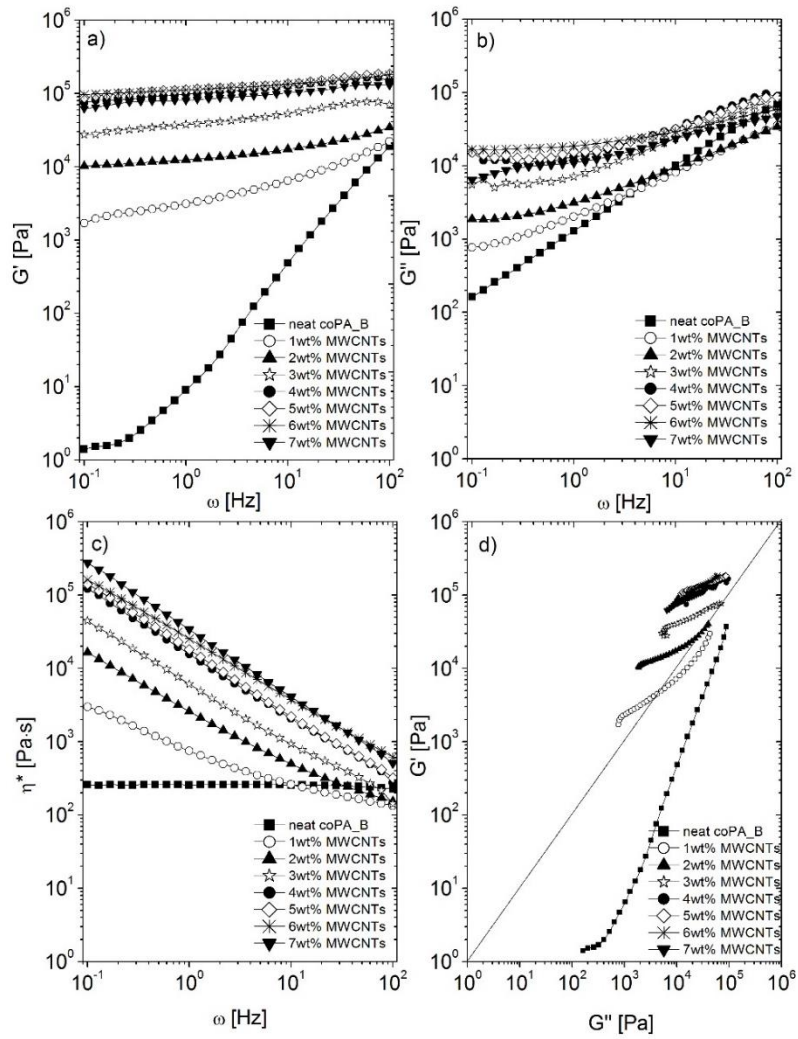


Figure 7: Variation in a) G' , b) G'' and c) complex viscosity (η^*) as a function of frequency and d) Cole-Cole plot.

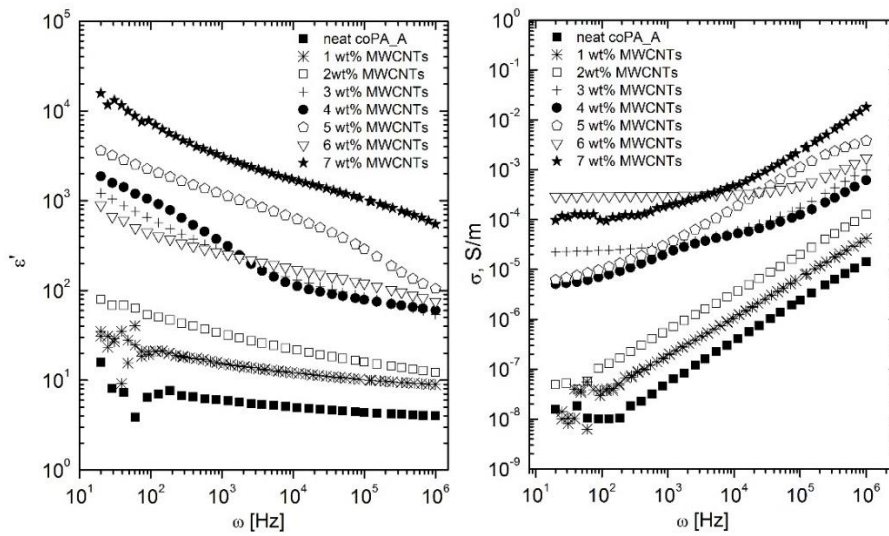


Figure 8: Frequency dependence of dielectric permittivity and electrical conductivity (AC) for composites of coPA_A and MWCNTs

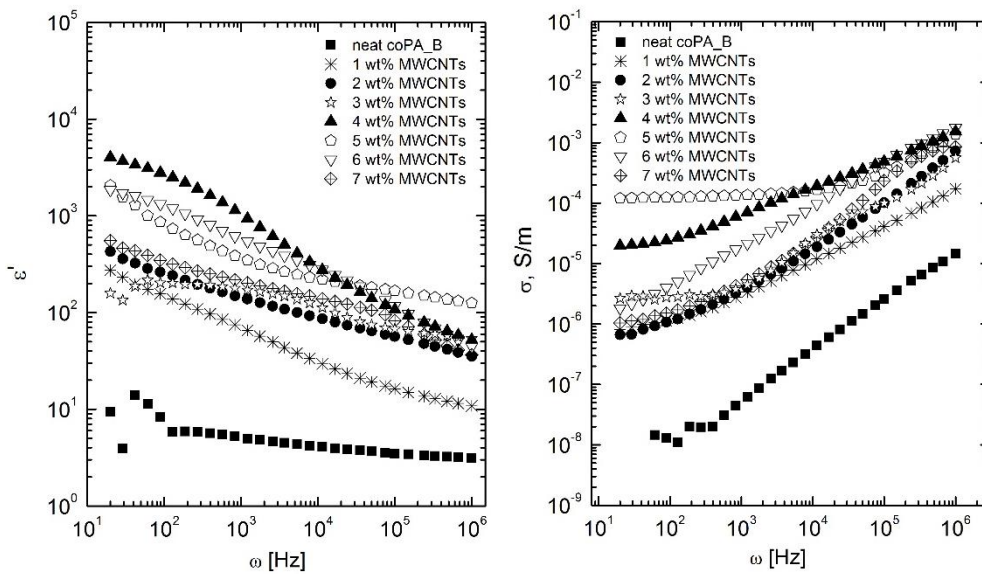


Figure 9: Frequency dependence of dielectric permittivity and electrical conductivity (AC) for composites of coPA_B and MWCNTs

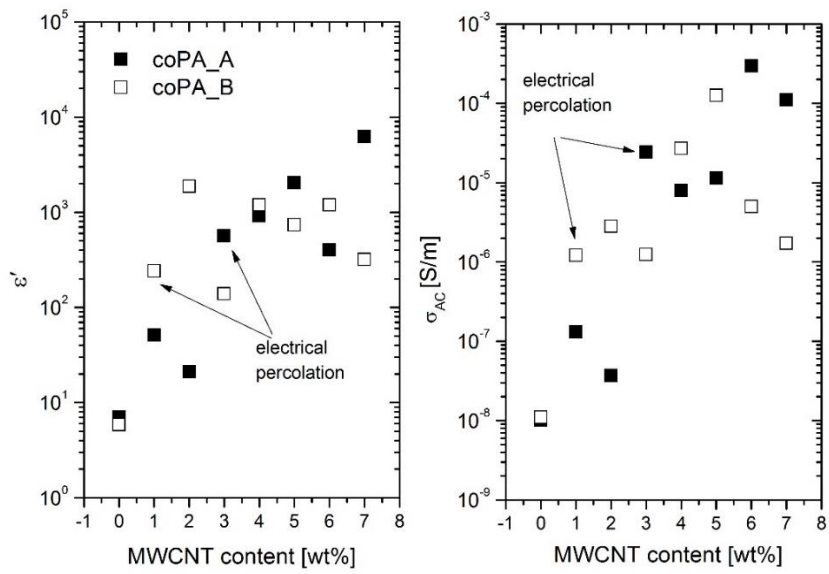


Figure 10: Concentration dependence of the dielectric permittivity and the electrical conductivity at 129 Hz in two types of hot melt copolyamides doped with MWCNT.

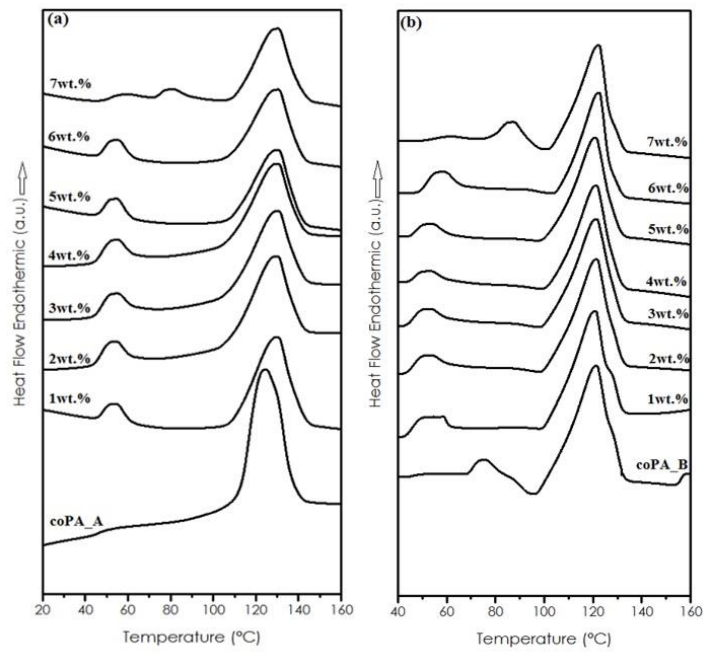


Figure 11. DSC first heating curves for (a) coPA_A based nanocomposites and (b) coPA_B based nanocomposites

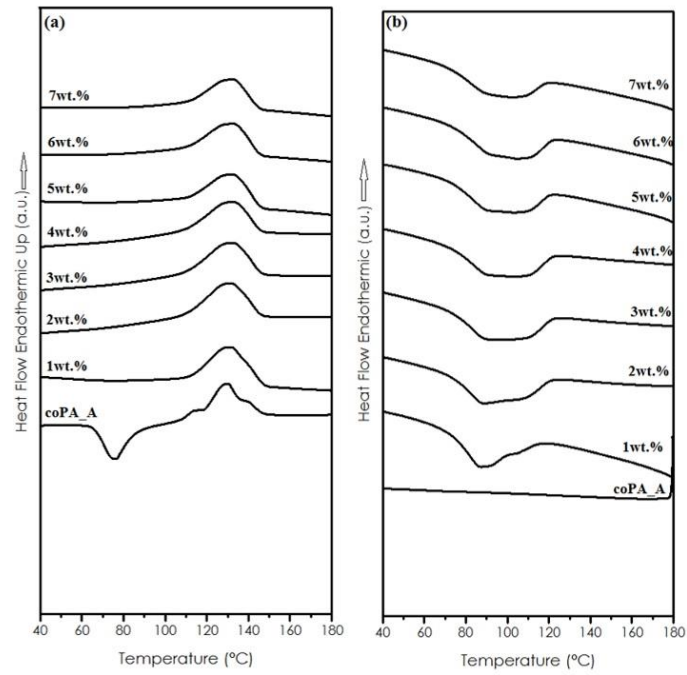


Figure 12. DSC (a) second heating and (b) cooling curves for unfilled coPA_A and composites of coPA_A and MWCNTs.

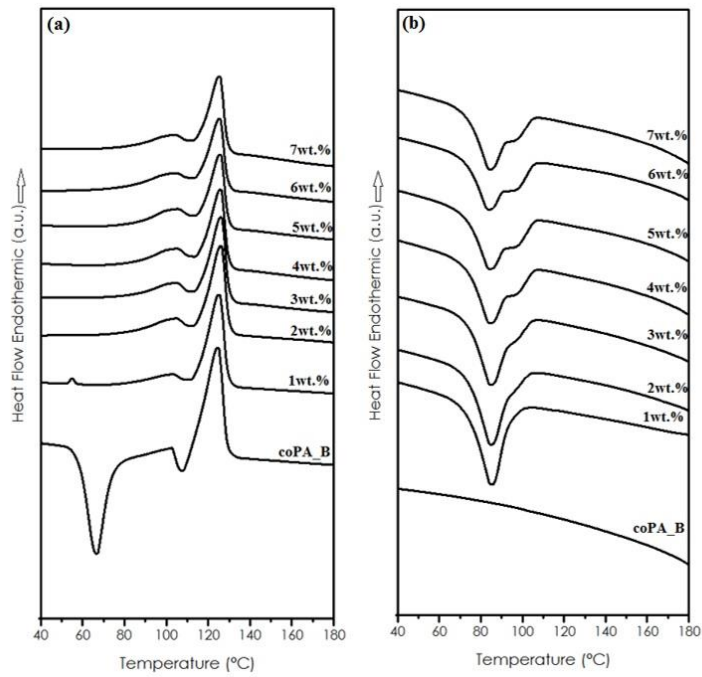


Figure 13. DSC (a) second heating and (b) cooling curves for unfilled coPA_B and composites of coPA_B and MWCNTs.

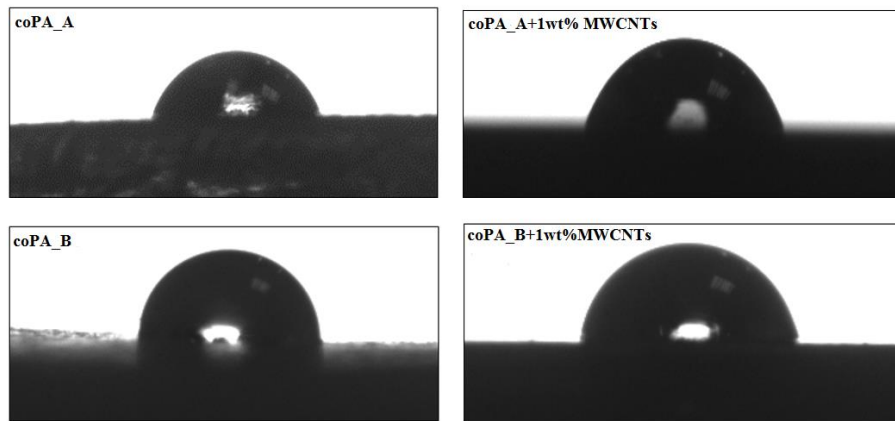


Figure 14. Images taken during contact angle measurements showing the effect of MWCNT addition on the wettability of the unfilled and MWCNT filled co-polyamides.

Table 1. General properties of the co-polyamides used in the study.

Co-polyamide (tradename)	Sample designation	Melt viscosity [Pa*s] 160°C/2.16kg	T _m [°C]
Griltex®D1330A	coPA_A	1200	125-135
Griltex®2A	coPA_B	600	120-130

Table 2. Thermal properties of coPA_A, coPA_B and composites of both co-polyamides with MWCNTs, from DSC measurements.

	1 st heating			2 nd heating		Cooling
	T _g [°C]	T _m [°C]	ΔH _m [J/g]	T _m [°C]	ΔH [J/g]	T _c [°C]
coPA_A neat	46.1	129	64.1	128	31.8	---
coPA_A+1wt%MWCNTs	48.5	130	41.1	132	32.3	86.7
coPA_A+2wt%MWCNTs	47.5	128	41.2	128	48.8	88.1
coPA_A+3wt%MWCNTs	48.1	127	42.3	129	46.8	90.2
coPA_A+4wt%MWCNTs	48.6	130	39.2	132	32.8	91.3
coPA_A+5wt%MWCNTs	47.6	130	34.2	133	29.8	90.9
coPA_A+6wt%MWCNTs	48.8	131	34.5	133	34.1	93.8
coPA_A+7wt%MWCNTs	51.4 75.8	131	32.3	133	29.0	93.1
coPA_B neat	70.6	121	51.9	124	40.4	---
coPA_B+1wt%MWCNTs	46.2	120	42.1	126	25.4	84.7
coPA_B+2wt%MWCNTs	46.5	121	42.9	126	23.2	84.5
coPA_B+3wt%MWCNTs	46.8	121	42.7	126	21.9	84.4
coPA_B+4wt%MWCNTs	46.9	122	39.0	126	19.6	84.0
coPA_B+5wt%MWCNTs	48.1	121	38.7	126	17.3	83.8
coPA_B+6wt%MWCNTs	51.8	123	32.3	126	17.3	83.5
coPA_B+7wt%MWCNTs	53.2 82.1	122	37.2	126	19.0	84

Table 3. Variation in contact angle and surface energy for coP_A, coPA_B and their composites with MWCNTs.

Material	Average contact angle [°]	Surface energy [mJ/m ²]
coPA_A	71.1 ± 5.61	41.19 ± 0.005
coPA_A+1wt% MWCNTs	70.1 ± 0.88	40.62 ± 0.002
coPA_A+2wt% MWCNTs	60.5 ± 1.88	41.65 ± 0.003
coPA_A+3wt% MWCNTs	66.3 ± 1.24	42.17 ± 0.003
coPA_A+4wt% MWCNTs	67.9 ± 1.52	43.01 ± 0.003
coPA_A+5wt% MWCNTs	68.1 ± 2.01	44.86 ± 0.002
coPA_A+6wt% MWCNTs	75.6 ± 3.38	38.29 ± 0.001
coPA_A+7wt% MWCNTs	68.8 ± 2.75	42.47 ± 0.006
coPA_B	96.9 ± 4.13	25.08 ± 0.004
coPA_B+1wt% MWCNTs	80.7 ± 2.49	35.09 ± 0.004
coPA_B+2wt% MWCNTs	67.5 ± 4.04	40.58 ± 0.012
coPA_B+3wt% MWCNTs	61.5 ± 5.44	47.68 ± 0.008
coPA_B+4wt% MWCNTs	66.6 ± 4.39	43.88 ± 0.005
coPA_B+5wt% MWCNTs	71.7 ± 4.09	40.72 ± 0.007
coPA_B+6wt% MWCNTs	70.3 ± 2.85	41.53 ± 0.007
coPA_B+7wt% MWCNTs	72.3 ± 3.99	39.41 ± 0.001